



Exosome Secretion Regulation in Mice with Acute Lung Injury

Hui-Hui Jie ^{1,2}, Wei-Hua Lu ^{1,3}

¹Department of Critical Care Medicine, The First Affiliated Hospital of Wannan Medical College (Yijishan Hospital of Wannan Medical College), Wuhu, Anhui, 241001, People's Republic of China; ²Graduate School of Wannan Medical University, Wuhu, Anhui, 241001, People's Republic of China; ³Anhui Province Clinical Research Center for Critical Respiratory Medicine, Wuhu, Anhui, 241001, People's Republic of China

Correspondence: Wei-Hua Lu, Department of Critical Care Medicine, The First Affiliated Hospital of Wannan Medical College (Yijishan Hospital of Wannan Medical College), No. 2 Zheshan Road, Wuhu, Anhui, 241001, People's Republic of China, Tel +86-13955370637, Email lwh683@126.com



Purpose: Acute lung injury (ALI) is a typical critical illness. Exosomes can regulate the development of pulmonary inflammation by modulating macrophage metabolism and behavior. During ALI, C—C motif chemokine ligand 2 (CCL2) is involved in the occurrence and maintenance of the inflammatory response, and the amount of CCL2 secreted by exosome increases. This study was aimed at investigating the role and mechanism of exosome —mediated CCL2 in sepsis—related ALI using a sepsis model in mice and rat type II alveolar epithelial cells. Furthermore, we explore the regulation of extracellular vesicle secretion in acute lung injury in mice.

Methods: The sepsis group was pretreated with an exosome inhibitor to determine the extent of exosome release and alterations in inflammatory factors in the lung tissue. Furthermore, RLE—6TN cell—derived exosomes were cocultured with rat alveolar macrophages. Subsequently, an ALI rat model was constructed, and exosomes produced in vitro were injected into rats via the tail vein to detect the expression levels of inflammatory factors and elucidate macrophage polarization pathways.

Results: After treatment with the exosome inhibitor, the number of exosomes and the expression of CCL2 in the lung tissue were significantly downregulated in the sepsis group. Exosomes secreted by lipopolysaccharide—treated rat type II alveolar epithelial cells stimulated the polarization of M1 macrophages, which resulted in morphological and functional changes.

Conclusion: Exosome Secretion Regulation in Mice with Acute Lung Injury.

Keywords: sepsis, C—C motif chemokine ligand 2, CCL2, exosome, lung macrophages, acute lung injury

Introduction

Acute lung injury (ALI) is a typical critical illness characterized by pulmonary hypoxia, with lipopolysaccharide (LPS) being one of the key causes.¹ Exosomes contain several bioactive substances sourced from their parent cells, such as RNA, DNA, proteins, and lipids, which can mediate intercellular communication and signal transduction.^{2,3} Many investigations have reported that Exosome can regulate pulmonary inflammation and injury by modulating macrophage metabolism and behavior.^{4,5} Alveolar macrophages are the first line of defense against invading pathogens that enter distal airways. Macrophages can be categorized into M1 and M2 types. M1 (classically activated) macrophages initiate and maintain the inflammatory response by secreting proinflammatory cytokines. Nonetheless, under certain conditions, such as in tumor microenvironments, they differentiate into anti— inflammatory M2 macrophages (alternatively activated). These block the release of proinflammatory stimuli and promote accelerated repair and the release of anti— inflammatory cytokines.⁶ Intercellular communication between macrophages and alveolar epithelial cells is essential for maintaining lung homeostasis. Macrophages are important innate immune cells involved in the inflammatory response of acute respiratory distress syndrome (ARDS).^{7,8}

CCL2 is a monocyte chemoattractant, and monocyte chemotaxis activator, and CCL2 plays a role in the migration of inflammatory cells, through the activation of integrins, increased levels of which are linked to severe lung injury and persistent inflammation in ARDS.⁹ CCL2 is a crucial chemokine released in the bronchoalveolar lavage of LPS—induced ALI mouse

models.¹⁰ During tissue injury, serum exosomes are secreted by various cell types, especially in cases of ALI/ARDS caused by excessive systemic inflammatory responses, such as sepsis—induced ALI.^{11,12} This study hypothesizes that sepsis can induce ALI, and increased exosome secretion and upregulated CCL2 expression in lung tissues may be the underlying mechanism. These changes lead to the polarization of lung macrophages to the M1 phenotype, increased release of inflammatory cytokines, and dysfunction of alveolar epithelial cells, which constitute the key mechanisms of ALI. The flow chart is given in Figure 1 below.

In this study, a mouse model of sepsis—induced ALI was established using cecal ligation and puncture. The role and mechanism of exosome—mediated CCL2 in sepsis—related ALI were examined using sepsis model mice and rat type II alveolar epithelial cells. The findings are expected to provide novel strategies to alleviate inflammation in patients with sepsis—related ALI.

Materials and Methods

Construction and Intervention of Mouse Sepsis ALI Model Male C57BL/6J mice (8–9 weeks old) were selected for this study (Zhejiang VITAL RIVER Laboratory Animal Technology Co, Ltd, SCXK (Zhe Jiang) 2019—0001). After adaptive feeding in a standard specific pathogen—free environment for 1 week, 24 mice were used in this study, with 6 animals per group. The grouping was as follows: Normal control (CT), sepsis (CLP), exosome inhibitor pretreatment sepsis (G+C), and

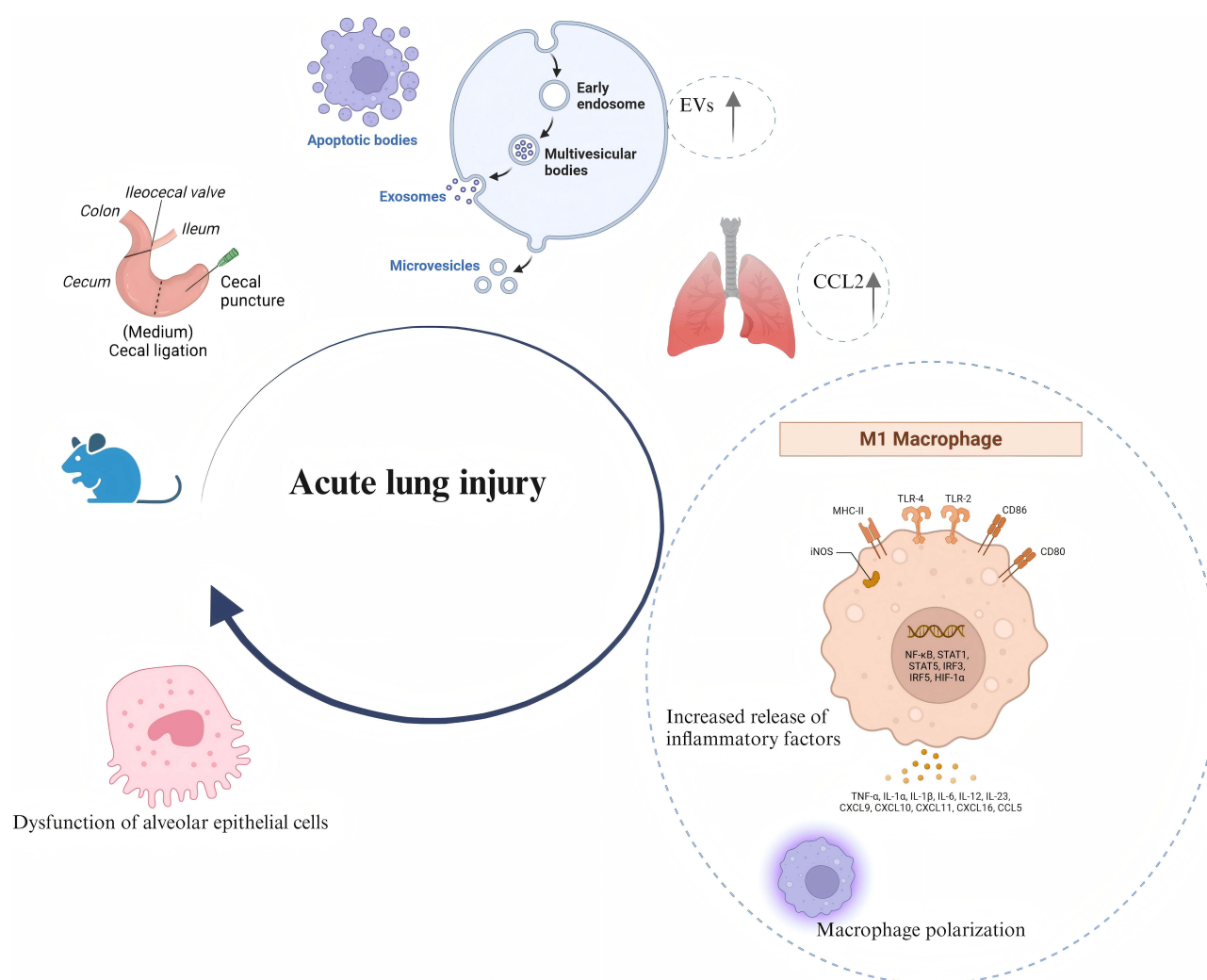


Figure 1 The flow chart. In this study, a mouse model of sepsis—induced ALI was established using cecal ligation and puncture. The role and mechanism of exosome—mediated CCL2 in sepsis—related ALI were examined using sepsis model mice and rat type II alveolar epithelial cells. The findings are expected to provide novel strategies to alleviate inflammation in patients with sepsis—related ALI.

exosome inhibitor (GW) groups. Mice in the CLP group were anesthetized with 0.3% pentobarbital sodium (30 mg/kg), shaved, disinfected with povidone–iodine, and a vertical midline incision was created on the abdominal wall. The cecum was exteriorized and ligated using a 4–0 silk at its base. Following ligation, the cecum was punctured twice with an 18–gauge needle and two drops of feces were squeezed out. The cecum was placed back into the abdominal cavity, and the incision was sutured in two layers.¹³ The G+C group was administered an intraperitoneal injection of the exosome inhibitor GW4869 [1.75 mg/kg dissolved in 0.1% dimethyl sulfoxide (DMSO)] 2 h before establishing the 36–h CLP model. On the contrary, the GW group was given an intraperitoneal injection of the exosome inhibitor GW4869 (1.75 mg/kg dissolved in 0.1% DMSO) (The 1.75mg/kg dose was determined by screening five exosome inhibitor dose gradient groups in preliminary experiments, as detailed in [Supplementary Material Figure 1](#)). Thirty–six hours after the modeling, lung tissues and plasma were collected from the mice for subsequent testing. 2mL of blood was used for the extraction of plasma exosomes. The blood collection process was for each group under 3% pentobarbital sodium anesthesia, and the mouse cavity was protruding and flattened, and the abdominal skin was gently pinched with the left hand, and used as the focal point. Holding 1 mL syringe, the right hand tip oblique up, about 10–20° Angle with the abdomen, from the junction of the xiphoid and the left costal arch, at this time, blood flow into the syringe. After seeing the blood, keep the syringe position still, draw the syringe backward at a uniform speed, keep the distance between the needle core and the blood plane about 0.1 mL, that is, there is a certain negative pressure, until the end of blood collection, pull out the syringe. When there was no more blood pump, the rat was killed by cervical dislocation, resting for 30min in 4°C, then centrifuged at 3000 rpm for 15min. After centrifugation, the supernatant was serum and carefully drawn with the pipette gun in 2mLEP tube (avoid absorbing the blood cells) for subsequent extraction of exosomes.

Comparison and Identification of Exosome Release Levels and Exosome Characterization in Four Groups

Particle size analyzer (Particle Metrix, ZetaView) and NTA were used for detection and data analysis, respectively. Imaging studies were performed using an electron microscope (HT7800/HT7700), and a Western blot (WB) was used to detect the exosome markers CD9 and CD63.

Isolation, Identification, and Quantification of Plasma Exosomes Using Real–Time Quantitative Polymerase Chain Reaction (qRT–PCR)

Exosomes were isolated using a four–step centrifugation method (2000 × g for 30 min at 4°C, 10,000 × g for 45 min, 100,000 × g for 70 min at 4°C, resuspended in 1× phosphate buffered saline, and recentrifuged at 100,000 × g for 70 min), followed by transmission electron microscopy (TEM, HITACHI, HT7800/HT7700) for imaging. Nano–flow cytometry (NanoFCM, N30E) was used to determine exosome particle size and concentration.

Exosome solutions were placed on copper grids coated with a continuous carbon film, incubated at room temperature for 1 min, washed with sterile distilled water, and stained using uranyl acetate solution (1%, m/v) for 1 min. The grids were blotted, further dried under an incandescent lamp for 2 min, and visualized and captured using a TEM (HITACHI, HT7800/HT7700).

RNA was extracted from the exosomes using the miRNeasy Mini Kit, and cDNA was synthesized using the RevertAid First Strand cDNA Synthesis Kit. Subsequently, qRT–PCR was performed using a fluorescence–based PCR instrument, which involved the following steps: predenaturation at 95°C for 10 min; denaturation at 95°C for 15s, annealing at 60°C for 20s, and extension at 72°C for 25s for 40 cycles; and final extension at 72°C for 5 min. The relative gene expression was calculated using the 2– $\Delta\Delta C_t$ method, for which cel–miR–39 served as the external reference. The primer sequences are listed in [Table S1](#).

Histopathology, Immunohistochemistry, and Western Blot

Lung tissue sections were deparaffinized, rehydrated, stained with hematoxylin for 3–5 min, washed, differentiated with 1% hydrochloric acid alcohol, blued with ammonia water, stained with eosin for 3–5 min, dehydrated, mounted, and observed under a microscope. Lung injury was scored based on the Smith scoring criteria.

Tissue sections were deparaffinized and rehydrated. The antigen was retrieved, and endogenous peroxidase activity was blocked. The sections were blocked and incubated with primary antibodies, and signals were detected using the Vectastain ABC kit (Vector Labs, Burlingame, CA, USA).

Exosome supernatants and lung tissue lysates were denatured and subjected to protein immunoblotting (15% sodium dodecyl sulfate—polyacrylamide gel electrophoresis). Polyvinylidene fluoride (PVDF) membranes were incubated with a supersensitive luminescent solution (RJ239676, Thermo Fisher) and imaged using an ultrasensitive chemiluminescence imaging system (Tanon—5200, Shanghai Tianneng Technology Co, Ltd). Antibody information is provided in [Table S3](#).

Cell Culture and Treatment

The origins of the primary rat macrophages and culture conditions.

Rat lung macrophage isolation: SD rats for 6–8 weeks, soaked the alcohol and exposed the trachea, ligated the upper end of the trachea, washed in PBS with a syringe, each repeated 3 times, irrigation fluid was collected, centrifuged at 2000rpm for 3min, cell precipitation was resuspended using 1640 complete medium, spread into the culture plate, and changed the next day.

Cell pavement: according to the experimental needs to cells in 48 well plate, 6 well plate, and the same method of cell passage, the cells according to the experimental needs for dilution, 48 well plate per well about 2104 cells, 6 well plate per well about 5105 cells, evenly spread in the cell culture plate, marking, placed in the incubator, cells completely attached after the experiment.

Preparation of exosome supernatant: the cells were cultured to 80%–90% density before LPS treatment. After the treatment, the cell supernatant was discarded, washed twice with PBS, replaced with incomplete 1640 medium, starved for 48h, and the supernatant was collected.

Rat type II alveolar epithelial cells RLE—6TN (iCell—r039, iCell) were cultured in RPMI1640 complete medium (KGM31800S, KeyGen Biotech) at 37°C in a 5% CO₂ incubator (Heraeus BB 150, Thermo Fisher). The optimal concentration of LPS was determined by randomly segregating the cultured rat macrophages into control and different LPS concentration groups (0, 25, 50, 100, 200, and 400 ng/mL). The cells were incubated for 24 h, and the optimal LPS concentration was used to extract the exosomes for further treatment and detection.

Enzyme—linked Immunosorbent Assay (ELISA)

ELISA was used to detect the expression levels of proinflammatory cytokines interleukin (IL)—6 and tumor necrosis factor (TNF)— α . Standard solutions were prepared according to manufacturer instructions. Blank, standard, and sample wells were set up, and 50 μ L of samples was added to each well, followed by 100 μ L of enzyme—labeled reagent. The samples were incubated at 37°C for 1 h, color development reagent was added, further incubated at 37°C for 15 min, and the reaction was terminated. The absorbance was read at 450 nm.

Exosome Extraction, Identification, and Quantification Using qRT—PCR

The exosome extraction process was rat type II alveolar epithelial cell RLE-6 TN (iCell-r039, iCell) 2000 g, 4°C, centrifuged for 30 min, the supernatant was transferred to a new centrifuge tube and centrifuged again at 10,000 g, 4°C, 45 min to remove larger vesicles. The supernatant was removed and filtered through a 0.45 μ m filter membrane to collect the filtrate. The filtrate was transferred to a new centrifuge tube and the overspeed rotor was selected and centrifuged at 4°C at 100,000 g for 70 min. The supernatant was removed and resuspended in 10 mL pre-cooled 1 PBS, the overspeed rotor was selected, again 4°C, 100,000 g, and overspeed centrifugation for 70 min. The supernatant was removed, resuspended in pre-cooled 1 PBS, 20 μ L EM, 10 μ L particle size, and stored the remaining exosomes at -80°C; (RLE-6 TN cells) for cell density to 80%–90%. Is the cell culture supernatant, Wash it twice with 1 PBS, Add 0.25% trypsin enzyme (containing 0.02% EDTA) for digestion, The cells were added to the media and the cell suspension was collected into a 10 mL centrifuge tube, Was centrifuged at 1000rpm for 3min, Remove the supernatant to the medium and resuspend the cells; The cell suspension was distributed in a 1:3 ratio to the prepared dish, Good marking, Place the cells in an incubator; After growing the cells to an 80–90% density, Conduct the LPS treatment, Cell supernatant was discarded at the end of treatment, Was washed 2 times using PBS, Replacement with an incomplete 1640 medium,

Starvation treatment for 48h, Supernatant (90mL) was collected from three T75 culture bottles.—step centrifugation method described above, and TEM (Hitachi, HT—7700) was used for imaging. Similarly, nano—flow cytometry (NanoFCM, N30E) was used to determine exosome particle size and concentration.

RNA was extracted from the exosomes using the miRNeasy Mini Kit, and cDNA was synthesized using the RevertAid First Strand cDNA Synthesis Kit. qRT—PCR was performed using a fluorescence—based PCR instrument using the following steps: predenaturation at 95°C for 10 min; denaturation at 95°C for 15s, annealing at 60°C for 20s, and extension at 72°C for 25s for 40 cycles; and final extension at 72°C for 5 min. The relative gene expression was calculated using the 2— $\Delta\Delta C_t$ method, and cel—miR—39 served as the external reference. The primer sequences are provided in [Table S2](#).

Immunofluorescence, Transwell Assay, Protein Immunoblotting, and Flow Cytometry

Rat lung macrophages were isolated, rat lung macrophages were spread with Transwell chambers, cells were laid to 48-well plates, then fixed with paraformaldehyde for 5–15min, and washed with PBS for 35 min. Cells were blocked using blocking solution for 30min, and primary antibody (rabbit anti-CD63 antibody, DF7518, affinity, 1:100) was combined. The temperature was incubated for 1h, and rinsed in PBST for 5min. Secondary antibody (horseradish peroxidase conjugated goat anti-rabbit IgG (H + L) (ZB-2301, ZSGB-1-200) was combined. The incubated 1h.PBST was rinsed 3 times at room temperature, after 5min of each rinse, and then once with distilled water. Sealing and testing. Add a drop of sealing tablet, and examine by fluorescence microscope (BX 53, OLYMPUS).

The cells were resuspended in serum—free medium and seeded in Transwell chambers. After 48 h of incubation at 37°C in the presence of CO₂, the chambers were removed, stained with 0.1% crystal violet (G1061, Solarbio) for 1 h, and examined microscopically (BX43, OLYMPUS). The absorbance was read at 562 nm using a microplate reader (WD—2012B, Beijing Six—One).

Total protein was extracted using RIPA lysis buffer, centrifuged at 12,000 r/min at 4°C for 10 min, and the supernatant was collected. The protein was quantified using a bicinchoninic acid assay kit (E—BC—K318—M, Elabscience), electrophoresed, and transferred to PVDF membranes (Millipore). The membranes were incubated with primary antibodies overnight and then with secondary antibodies. Subsequently, the membranes were soaked in super-sensitive luminescent solution (RJ239676, Thermo Fisher) and imaged using an ultrasensitive chemiluminescence imaging system (Tanon—5200, Shanghai Tianneng Technology Co., Ltd). Antibody information is furnished in [Table S4](#).

The cells (1 × 10⁶) were collected, and washed twice by centrifugation at PBS 1500 rpm for 3 min; 300 μ L of pre-cooled 1 Annexin V-FITC binding solution and 5 μ L Annexin V-FITC (AP-101-100-kit, MULTI SCIENCES) and 10 μ L PI to each well. After slight mixing, the cells were incubated at room temperature for 10 min and tested by flow cytometer.

Construction and Intervention of Rat Sepsis ALI Model

Six—week—old male SD rats (Beijing HuaFuKang Bioscience Co., Ltd., license number: SCXK (Jing) 2019—0008) were adaptively fed in a standard specific pathogen—free environment for 1 week. Nine rats were randomly categorized into the following groups: Control, LPS, and LPS+EXO groups (three rats per group). The rats in the LPS and LPS+EXO groups were anesthetized with 3% pentobarbital sodium, shaved, placed in the supine position, disinfected with iodine, and subcutaneous tissues were dissected to expose the trachea. Subsequently, LPS (1 mg/kg) was injected intratracheally with a 1 mL syringe. Exosome solutions (20 μ g) were injected into the tail veins of the LPS+EXO group rats after 6 h of modeling. Plasma and lung tissues were collected from the rats for testing.

Histopathology, Immunohistochemistry, and Immunofluorescence Double Staining

Sections of the right upper lobe of the rat lung were baked, deparaffinized, and hydrated for histopathological analysis. In the next step, they were stained with hematoxylin (ZLI—9610, ZSGB—Bio) for 3–5 min, washed with running water, differentiated with 1% hydrochloric acid alcohol, blued with ammonia water, and then stained with eosin (G1100, Solarbio) for 3–5 min. Later, they were dehydrated, mounted, and examined microscopically (BX43, Olympus).

For immunohistochemical analysis, sections of the right upper lobe of the rat lung were baked, deparaffinized, and hydrated. Antigen retrieval was performed using citric acid buffer. The sections were then blocked with 5% bovine serum

albumin (BSA) and incubated with the primary antibody (rabbit anti—CD68 antibody, DF7518, Affinity, 1:100) overnight at 4°C. In the subsequent step, they were incubated with the secondary antibody, ie, horseradish peroxidase—conjugated goat anti—rabbit IgG (H+L) (ZB—2301, ZSGB—Bio, 1:100). Diaminobenzidine was used for color development, and hematoxylin was employed for counterstaining. The sections were dehydrated, cleared, mounted, and observed microscopically (BX43, Olympus).

Immunofluorescence double staining was then performed, for which paraffin sections of the right upper lobe of the rat lung were baked, deparaffinized, and hydrated. As mentioned previously, antigen retrieval was performed using citric acid buffer. After blocking with 5% BSA, the sections were incubated with the primary antibody (rabbit anti—CD68 antibody, DF7518, Affinity, 1:300) overnight at 4°C, washed, and then incubated with the secondary antibody (horseradish peroxidase—conjugated goat anti—rabbit IgG (H+L) (ZB—2301, ZSGB—Bio, 1:200)) and CY3—Tyramide (G1223, Servicebio, 1:1500) at 37°C for 10 min. Again, the sections were blocked with 5% BSA, incubated with the second primary antibody [rabbit anti—inducible nitric oxide synthase (i—NOS) antibody, AF0199, Affinity, 1:200] overnight at 4°C, washed, and incubated with the second secondary antibody (goat anti—rabbit IgG/488 (ZF—0511, ZSGB—Bio, 1:100)) at 37°C for 45 min. Finally, the sections were counterstained with 4',6—diamidino—2—phenylindole, mounted, and observed under a fluorescence microscope (BX53, OLYMPUS).

Statistical Analysis

Statistical analysis was performed using GraphPad Prism 8.0.2 and ImageJ software. The *t*—test was used for comparisons between two groups and analysis of variance for multiple group comparisons. A *p*—value of <0.05 was considered statistically significant.

Results

Establishment of Sepsis Model and Comparison of Exosome Release and Identification

WB analysis confirmed that the sepsis—induced ALI model was successfully developed in mice. Compared with the CT group, the CLP group exhibited significantly increased expressions of TNF— α , IL—6, and CCL2 proteins (Figure 2A—D). The optimal dose of GW4869 for inhibiting exosome release in the plasma of septic mice was determined to be 1.75 mg/kg via NTA (Figure 2G). Furthermore, TEM was used to observe the typical morphology of EVs obtained from each group (Figure 2E). Exosome marker proteins CD9 and CD63 were present in all groups (Figure 2F). The exosome concentration was measured using a particle size analyzer (Particle Metrix, ZetaView). The exosome concentration increased during sepsis, but the application of the exosome inhibitor downregulated it in the sepsis group (Figure 2G).

Analysis of Inflammatory Factor Expression in Exosomes After the Inhibition of Their Release

TEM was used to determine the morphology of EVs obtained from each group (Figure 3A). The particle size, concentration, and surface protein expression positivity rate of the exosomes were estimated using nano—flow cytometry (Figure 3B and C; * indicates that the values were significantly different at *P* < 0.05 in comparison with the CT group). To evaluate the expressions of inflammatory factors TNF— α , IL—6, and CCL2 in the exosomes after the inhibition of their release, qPCR was performed. As illustrated in Figure 3D, the expressions of these inflammatory cytokines were downregulated in the exosomes of the sepsis group after release inhibition.

Inhibition of Exosome CCL2 Release and its Effect on ALI in Sepsis Mice

Histological analysis of lung tissues and lung injury scores indicated that the CLP group showed considerable alveolar wall thickening, narrowed alveolar spaces, extensive inflammatory cell infiltration, multiple hemorrhagic areas, and pronounced alveolar expansion. On the contrary, the pathological damage was alleviated in the G+C group (sepsis + exosome inhibitor) compared with the CLP group (Figure 4A). Immunohistochemical analysis of lung tissues signified the elevation of CCL2 expression in the CLP group compared with the CT group, whereas the G+C group exhibited decreased CCL2 expression compared with the CLP group (Figure 4B). In addition, WB analysis demonstrated that TNF— α , IL—6, and CCL2 protein

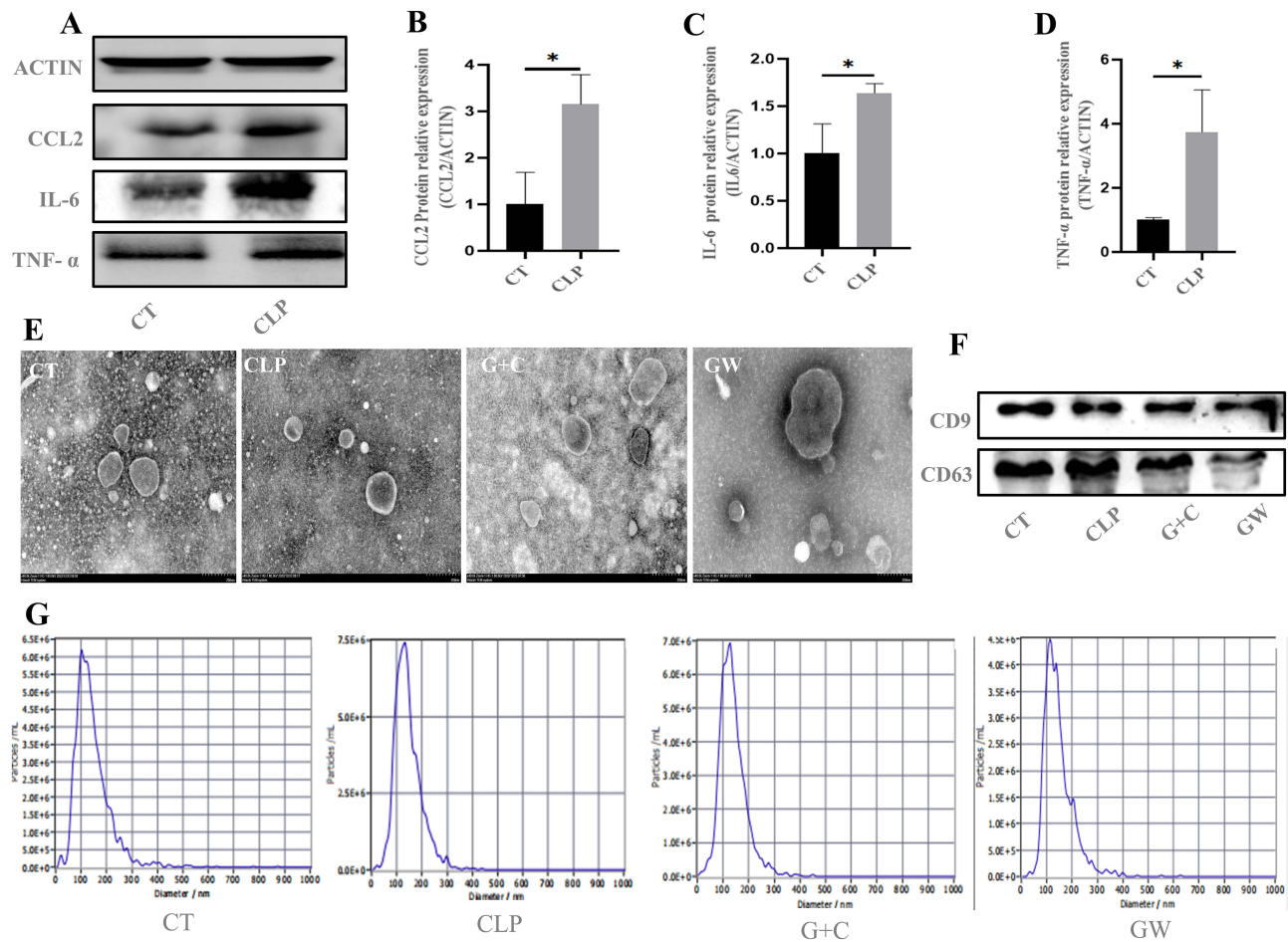


Figure 2 Inhibition of Exosome Release and Identification of Plasma Exosomes in the Sepsis Group. **(A)** Detection of protein expression in the lung tissues ($n = 3$). **(B–D)** Quantitative analysis of the protein content (* $P < 0.05$ compared to the Control group). **(E)** TEM micrographs of lung tissue exosomes isolated from each group of mice. **(F)** WB of exosome marker proteins CD9 and CD63 in the lung tissues. **(G)** NTA displaying the concentration and size distribution of lung tissue exosomes in each group ($n = 6$). **Abbreviations:** CT, Control group; CLP, Sepsis group; G+C, Sepsis + Exosome inhibitor group; GW, Exosome inhibitor group.

levels were significantly higher in the CLP group than those in the CT group. Conversely, the G+C group displayed reduced levels of these proteins compared with the CLP group (Figure 4C–F).

Analysis of CCL2 Expression in Exosomes from LPS—treated RLE—6TN Cells

Supernatants and lysates from lps-treated RLE-6 TN cells were collected and IL-6 and TNF- α levels in the supernatants were measured using ELISA (Figure 5A and B). In addition, we also measured the levels of inflammatory cytokines in the RLE-6 TN cell lysates by ELISA (Figure 5C and D). Based on the results of this comprehensive analysis, 100 ng/mL was selected as the optimal concentration for subsequent experiments. The exosomes were isolated from RLE—6TN cells via ultracentrifugation, and their morphology was observed via TEM. The findings revealed typical structures, with diameters in the range of 30–150 nm and characteristic bilayer membrane structures (Figure 5E). When particle size, concentration, and surface protein expression of the exosomes were measured using nano—flow cytometry, the average particle sizes were found to be 83 nm and 88.4 nm and the concentrations were 9.41×10^9 particles/mL and 8.55×10^9 particles/mL, respectively. The surface protein expression positivity rates were 7.9% and 16.9% for CD9 and 3.3% and 6.4%, respectively, for CD63 (Figure 5F and G). RT—qPCR was used to detect CCL2 expression in the exosomes secreted by rat type II alveolar epithelial cells in each group, which showed that it was significantly higher in the LPS group than that in the control group (Figure 5H).

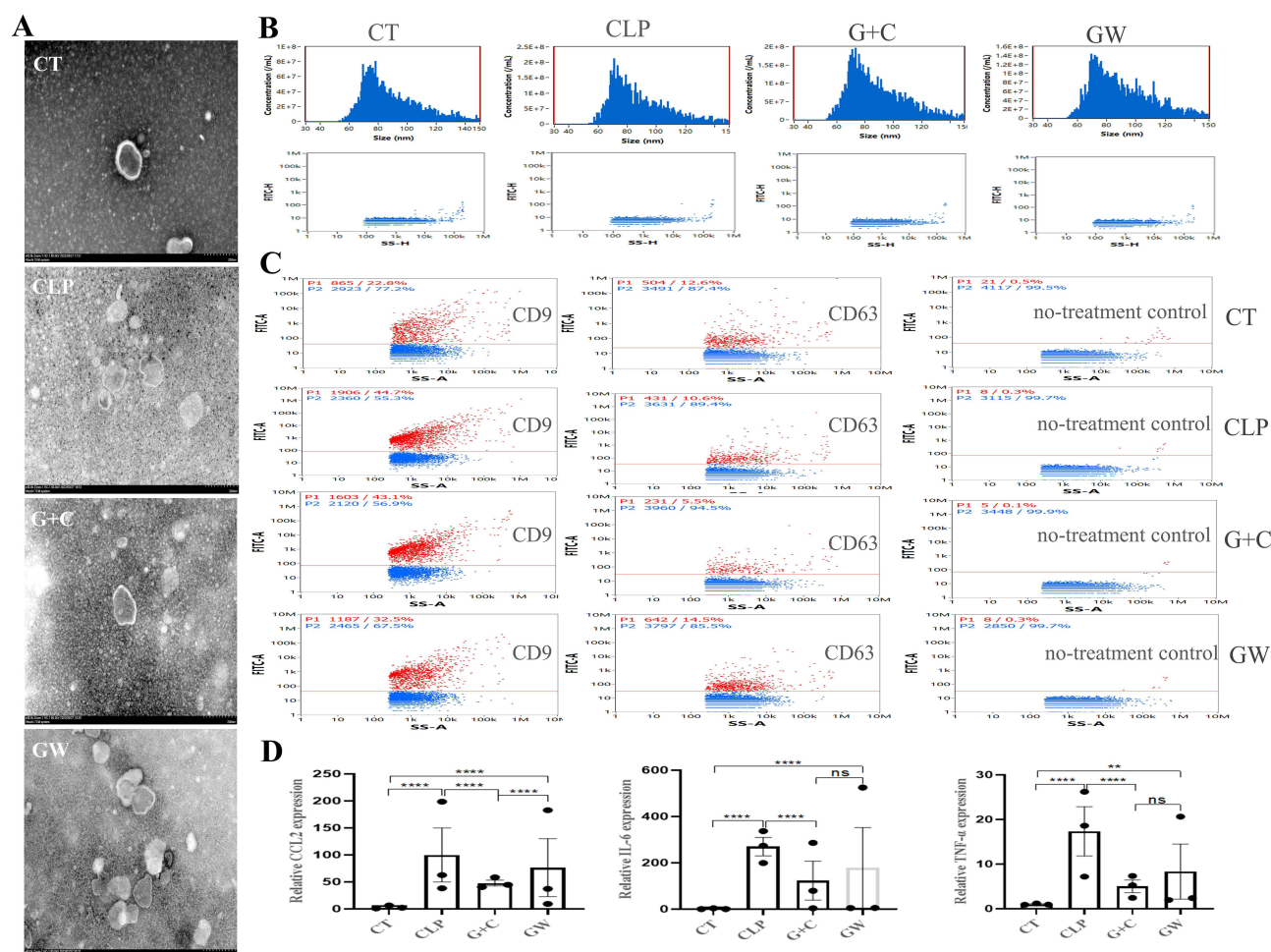


Figure 3 Identification of Plasma Exosomes and Inhibition of Inflammatory Factors in Exosomes. **(A)** TEM micrographs of exosomes isolated from the plasma of each group of mice ($n = 6$). **(B and C)** Nanoflow cytometry analysis of exosome particle size, concentration, and surface protein expression positivity rate. **(D)** qPCR detection of inflammatory factors TNF- α , IL-6, and CCL2 expression in the exosomes from each group ($n = 6$) (** $p < 0.01$, the results are highly statistically significant; **** $P < 0.0001$ compared to the Control group, the results are statistically highly significant).

Effect of RLE—6TN Cell Exosomes on the Polarization of Rat Alveolar Macrophages

Immunofluorescence staining showed that the exosomes were positive for the CD63 protein in rat lung macrophages (Figure 6A). Primary rat lung macrophages were cultured with exosomes (50 $\mu\text{g/mL}$) for 0, 24, and 48 h, with the control group receiving complete medium. Transwell migration experiment suggested that RLE—6TN cell exosomes significantly promoted the migration of rat alveolar macrophages at 24 h. however, at 48h, there was no significant difference in cell migration between the EXO and LPS+EXO groups and the Control group.(Figure 6B–D). Subsequently, supernatants were collected from primary rat lung macrophages treated with varying concentrations of LPS, and ELISA was performed to estimate IL—6 and TNF— α levels. The findings revealed that compared with the control, LPS treatment significantly augmented IL—6 and TNF— α levels. This effect was most pronounced at 400 ng/mL; hence, this concentration was selected for subsequent experiments (Figure 6E and F). ELISA of supernatants from primary rat lung macrophages showed the significant elevation of IL—6 and TNF— α levels in the LPS group compared with the control group. The LPS+EXO group exhibited even higher levels of IL—6 and TNF— α compared with the LPS group (Figure 6G and H). WB analysis demonstrated that i—NOS, Arg1, and TNF— α protein levels were higher in the LPS group than those in the control group. Arg1, and TNF— α levels were further elevated and IL—1 β levels were reduced in the LPS+EXO group compared with the LPS group (Figure 6I–M). Flow cytometry analysis suggested that CD86 protein levels were higher in the LPS group than those in the control group, whereas CD163 and CD206 protein levels were

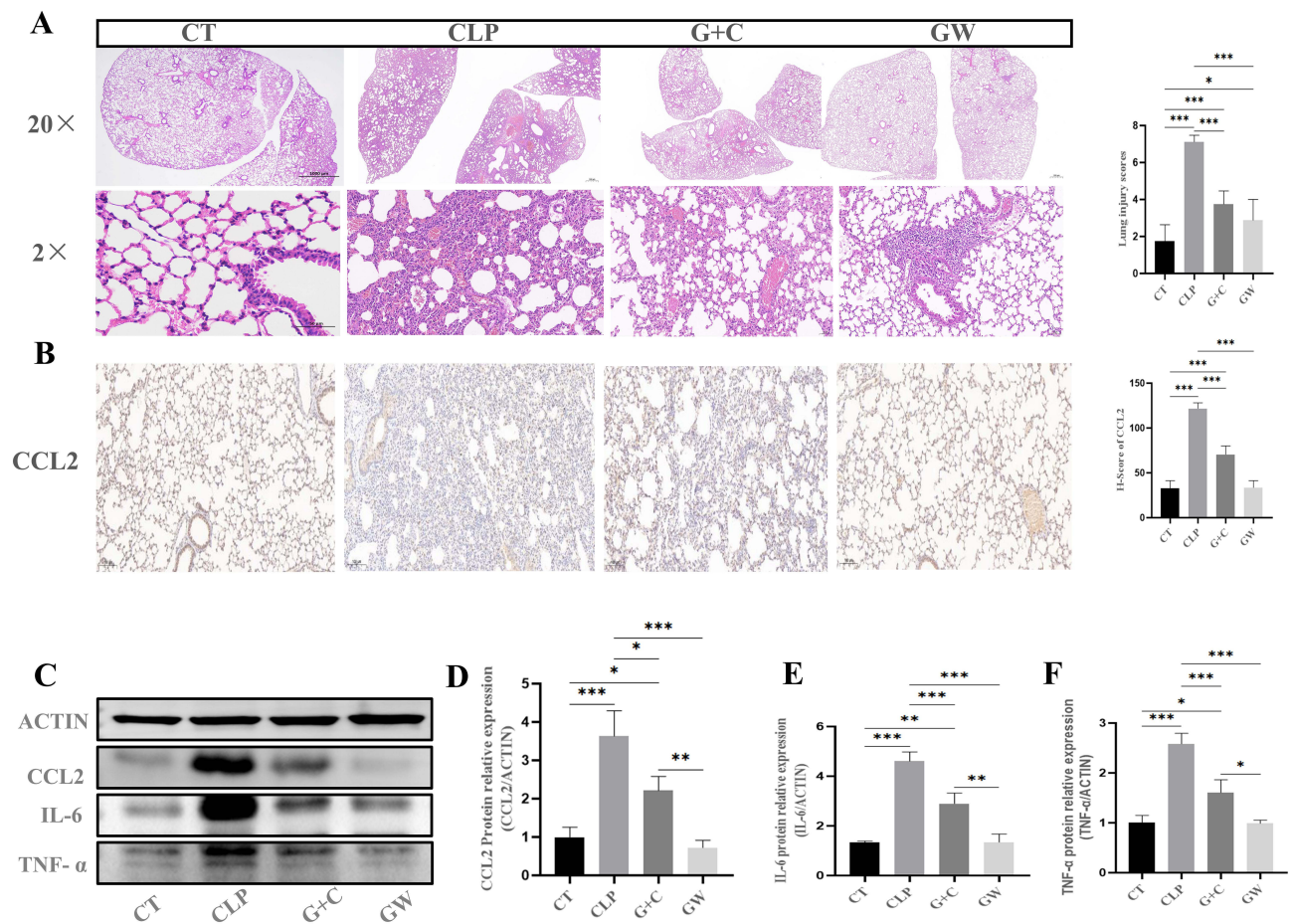


Figure 4 Inhibition of Exosome CCL2 Release Alleviates ALI. **(A)** Histopathological analysis of the lung tissues. HE staining and lung injury scoring were used to evaluate the inflammation in mouse lungs 36-h post-CLP modeling ($n = 8$). **(B)** IHC detection of the CCL2 expression in the lung tissues ($n = 8$). **(C)** Western blotting analysis of CCL2 protein in the lung tissues ($n = 3$). **(D–F)** Quantitative analysis of the protein levels. (* $p < 0.05$, the results are statistically significant; ** $p < 0.01$, the results are highly statistically significant; *** $p < 0.001$, the results are highly statistically significant).

lower. In contrast, the LPS+EXO group showed decreased CD86 levels and increased CD163 and CD206 levels compared with the LPS group (Figure 6N and O).

Analysis of the Effect of RLE—6TN Cell Exosomes on ALI in Sepsis Rats

Hematoxylin and eosin staining of the right upper lobe of the rat lung indicated that the LPS+EXO group exhibited more pronounced thickening of the alveolar septa, alveolar rupture and fusion, localized inflammatory foci, and increased hemorrhage than the LPS group (Figure 7A). Immunohistochemical analysis revealed that RLE—6TN cell exosomes upregulated CD68 expression in the lung tissues of sepsis rats (Figure 7B). Furthermore, dual immunofluorescence staining of the right upper lobe of the rat lung established that RLE—6TN cell exosomes induced the upregulation of i—NOS and CD68 expression in sepsis rat lung tissues (Figure 7C).

Discussion

Patients with sepsis often succumb to excessive inflammation triggered by immunosuppression or primary infections, and a high mortality rate is seen in those with sepsis—induced ALI.^{14–17} CCL2 (MCP—1) serves as a biomarker to predict sepsis.¹⁸ During inflammation, monocytes, macrophages, and vascular endothelial cells secrete MCP—1, which chemotactically activates monocytes/macrophages in a specific manner.¹⁹ CCR2 has been reported to be considerably over-expressed in macrophage and primary alveolar macrophage models induced by LPS in ARDS.²⁰ The results of qPCR obtained from our study, which showed significantly elevated CCL2 expression in the LPS group compared with the

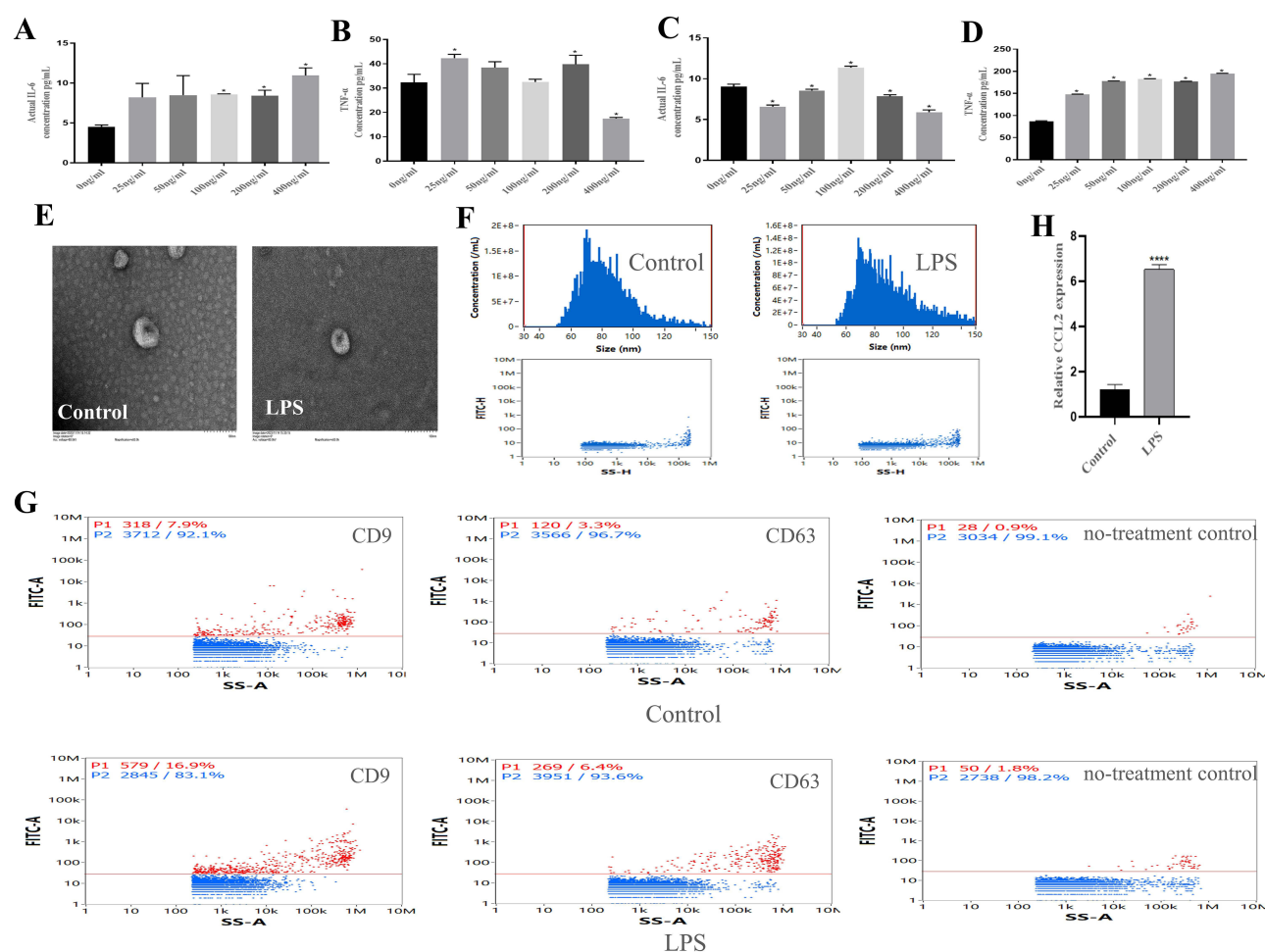


Figure 5 Upregulation of CCL2 Expression in Exosomes Induced by LPS Treatment of RLE-6TN Cells. (**A** and **B**) Comparison of the inflammatory cytokine levels in the supernatants of RLE-6TN cells treated with different LPS concentrations. (**C** and **D**) Comparison of the intracellular inflammatory cytokine levels in RLE-6TN cells treated with different LPS concentrations (* $P < 0.05$ compared to the Control group). (**E**) TEM observation of exosome morphology. (**F** and **G**) Nanoflow cytometry analysis of exosome particle size, concentration, and surface protein expression positivity rates. (**H**) qPCR analysis of the CCL2 levels in exosomes ($n = 3$) (**** $P < 0.0001$ compared to the Control group, the results are statistically highly significant).

control group, are aligned with previous findings. Multiple upregulated differentially expressed genes were identified in the ALI/ARDS related datasets, including CCL2. Enrichment analysis indicated that the expression of CCL2 in the LPS group model was in excess of the control group.²¹ Alveolar macrophages, the most abundant phagocytes in the alveolar space, are intricately involved in ALI. The dysfunction of the alveolar endothelial/epithelial barrier is a major contributing factor.²² Recruitment is a critical determinant that maintains the number of macrophages at inflammation and immune sites, with monocyte attractants such as CCL2/MCP-1 playing crucial roles.^{23,24}

Investigations have documented the role of macrophages in releasing chemokines such as MCP-1, which enhance the recruitment of neutrophils and monocytes to the lungs.^{25,26} Exosomes are known for their role in inducing proinflammatory effects, and studies are being focused on their involvement in lung injury and inflammation. Alveolar structural cells secrete Exosomes, which may either exacerbate or mitigate pulmonary inflammation.^{27,28} The finding that exosomes are natural carriers of functional small RNAs and proteins has attracted tremendous interest in drug delivery. Exosomes hold promising potential for the therapeutic delivery of miRNA, siRNA, mRNA, peptides, and synthetic drugs.²⁹

A study has opined that a cytokine network involving IL-6, IL-8, MCP-1, and IL-10 might play a pivotal role in the acute phase of sepsis.³⁰ Therefore, whether exosome inhibitors could alleviate ALI was investigated in this study by examining the protein expression levels of CCL2, IL-6, and TNF- α . Various cell types, including macrophages, monocytes, and endothelial cells, can secrete CCL2.³¹ Exosomes concentrations in pulmonary edema fluid from patients with

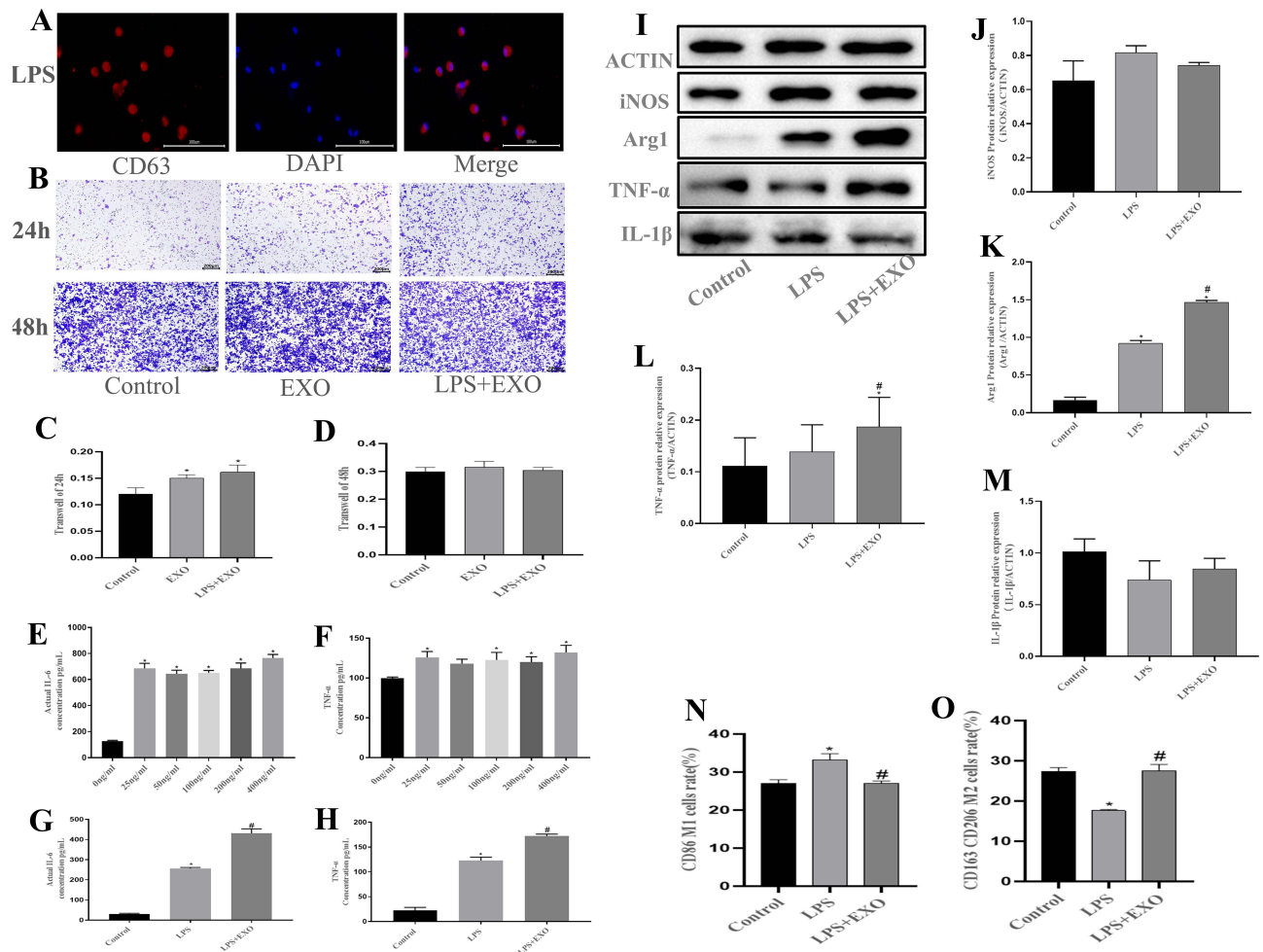


Figure 6 RLE—6TN Cell Exosomes Enhance M1 Polarization of Lung Macrophages. (A) Immunofluorescence staining of primary rat lung macrophages. (B—D) Crystal violet staining and quantitative analysis of primary rat lung macrophages in a Transwell assay ($n = 3$) (* $P < 0.05$ compared to the control group). (E and F) ELISA analysis of inflammatory cytokines in the supernatant of primary rat lung macrophages treated with different concentrations of LPS to determine the optimal concentration for inducing inflammatory cytokine production. (G and H) ELISA analysis of the effect of rle-6TN cell-derived exosomes on inflammatory cytokines in the supernatant of lung macrophages under the optimal dose of LPS. (I) WB analysis of polarization markers in macrophages ($n = 3$). (J—M) Quantitative analysis of the protein levels. (N and O) Flow cytometry analysis of the effect of RLE—6TN cell exosomes on lung macrophage polarization (Control: normal control group; LPS: LPS group; LPS+EXO group: LPS + alveolar epithelial cell exosomes) (* $P < 0.05$ compared to the control group; # $P < 0.05$ compared to the LPS group).

ARDS are higher than those in control subjects, and significant Exosomes secretion is noted in the bronchoalveolar lavage fluid following lung infection or injury.³² As resident professional phagocytes, alveolar macrophages can internalize microvesicles, which leads to pulmonary inflammation—a common pathological feature in alveolar inflammation, particularly in ARDS.³³ Macrophages are recipient cells of exogenous exosomes, with recent studies indicating that peripheral serum exosomes promote M1 macrophage polarization and inflammation during sepsis—associated ALI; however, the cellular origin of circulating exosomes has not been addressed.⁴ This study alludes that the use of exosome—mediated inflammatory factors is a novel therapeutic direction for ALI. CCL2 is a crucial chemokine released in bronchoalveolar lavage in LPS—induced ALI mouse models.²⁰ Our study observed that exosome inhibitors significantly reduced the expressions of cytokines CCL2, TNF— α , and IL—6 in sepsis—associated ALI in mice. This finding indicates that exosome—mediated CCL2 plays a pivotal role in the mechanism of sepsis—associated ALI.

Various stimuli can induce macrophage polarization states, with LPS being common, and the expressions of genes encoding i—NOS and ARG1 are used to define classically activated M1 (i—NOS) and alternatively activated M2 (ARG1) macrophages.³⁴ Epithelial cells and macrophages are the first line of defense in lung injury and inflammation.²⁶ Lung macrophages polarize into the M1 type during the acute exudative phase of ALI/ARDS, which provides reactive oxygen

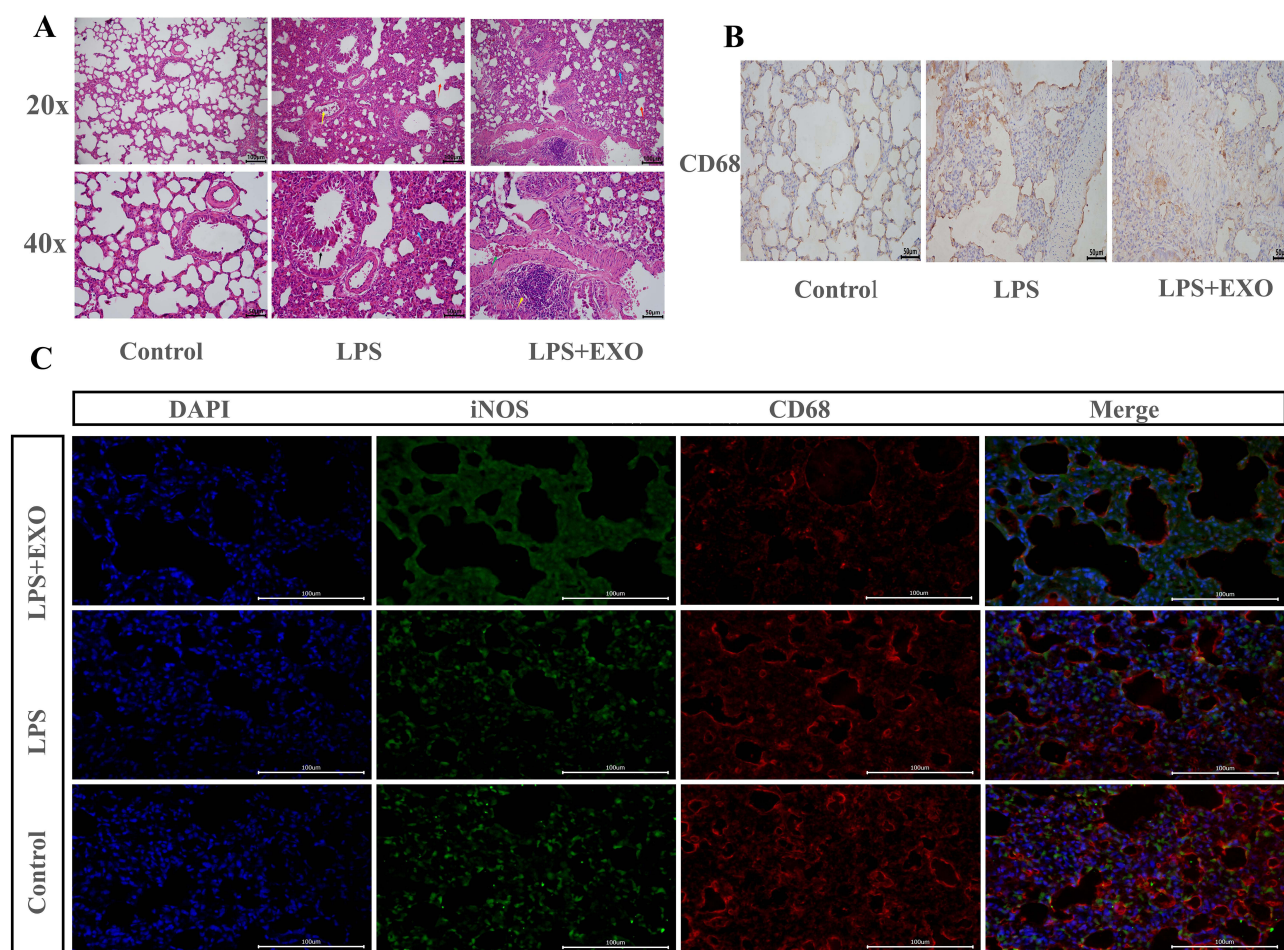


Figure 7 RLE—6TN Cell Exosomes Induce Macrophage Polarization and Exacerbate Lung Injury in Sepsis Rats. **(A)** CD68 expression (n = 3). **(B)** Immunohistochemical detection of the = 3). **(C)** Comparison of i—NOS and CD68 protein expression in the lung tissues by dual immunofluorescence staining (Control: normal control group; LPS group; LPS+EXO group: LPS + alveolar epithelial cell exosomes).

species (ROS), nitric oxide, IL—1, and TNF— α to enhance inflammatory responses. M2 macrophages are key regulators in the recovery phase and are involved in lung injury and tissue repair. Imbalances in M1/M2 polarization may induce excessive proinflammatory cytokine production and aggravate inflammation. Thus, controlling macrophage polarization may aid ALI prognosis.³⁵ M1 macrophages produce pro-inflammatory cytokines such as IL-1 β , iNOS, TNF- α , IL-1, IL-6, IL-12, IL-23, CCL8, CXCL1-3, CXCL-5, CXCL8-10, MCP-1, MIP-2, ROS, and COX-2, leading to pro-inflammatory responses, chemotaxis, pathogenic microorganism elimination, and antitumoral activities. M2 macrophages are induced in response to Th2 cytokines such as macrophage colony-stimulating factor (M-CSF), IL-4, IL-13, and IL-10. M2 macrophages mainly express CD64 and CD209 and produce anti-inflammatory cytokines such as IL-8, IL-10, IL-13, CCL1, CCL2, CCL3, CCL4, CCL13, CCL14, CCL17, CCL18, CCL22, CCL23, CCL24, and CCL26 to exert anti-inflammatory effects, promote tissue remodeling, facilitate tumor development.³⁶

A study has summarized that CCL22, IL—12B, IL—1 β , IL—6, i—NOS, and TNF— α are the upregulated markers common to M1 and M2 polarization phenotypes.³⁷ Hence, examining macrophage markers, such as ROS, TNF— α , i—NOS, and ARG1, can help in determining the occurrence of macrophage polarization.

In our in vitro study, RLE—6TN cell—derived exosomes obtained via ultracentrifugation were used to culture and stimulate primary rat lung macrophages in various groups. Scratch assays suggested considerable macrophage migration in the EXO and LPS+EXO groups compared with the control group. IL—1 β and TNF— α are two key proinflammatory cytokines.³⁸ Our WB results showed that exosome—induced macrophages significantly enhanced the secretion of inflammatory mediators and chemokines, such as Arg1 and TNF— α ; Furthermore, ELISA results indicate an increase

in IL-6 and TNF- α . An interesting phenomenon was observed in the ELISA experiment. During the LPS dose selection experiment, we saw that the amount of IL-6 was approximately 700 pg/mL, whereas after exposure to the same concentration of LPS, we only observed about 300 pg/mL of IL-6. Regarding this issue, we considered the possible reason that the morphology and function of macrophages are variable. Even though we ensured consistency in culture and extraction conditions in the experiment, each cell's absorption and metabolism of the drug are different.

Flow cytometry analysis revealed the elevated expressions of CD163 and CD206 proteins. Importantly, flow cytometry and WB results signified that both M1 and M2 polarization were enhanced. Although the expression of CD86 in the flow cell results chart did not increase but decreased, our explanation of this phenomenon is that the relevant literature has summarized the phenotype characteristics of human and murine macrophages, and CD86 was expressed in M1 and M2 in the phenotype characteristics of murine macrophages.³⁹ Macrophage M1 polarization can secrete the pro-inflammatory representative factors IL-6 and TNF- α . In our experiments, increased TNF- α expression in WB and increased IL-6 and TNF- α expression in ELISA could conclude that macrophage M1 polarization occurred. In the in vivo validation experiments, increased CD68 expression and HE staining in the immunohistochemical and double immunofluorescence staining results suggested that RLE-6 TN cell-derived exosomes induced M1 polarization in macrophages, which aggravated the lung injury in septic rats.

Therefore, the findings from this study have established that inhibiting exosome-mediated CCL2 release in sepsis mice alleviates ALI. Exosomes secreted by LPS-treated rat type II alveolar epithelial cells can activate macrophages and alter their morphology and function. Thus, exosome-mediated CCL2 regulates the M1 polarization of macrophages and promotes sepsis-associated ALI.

Nonetheless, this study has certain limitations, including a small sample size and a primary focus on macrophage M1 polarization without examining potential M1 to M2 polarization transitions.

Conclusion

Our research results indicate that sepsis can induce ALI, with increased exosome secretion and upregulated CCL2 in the lung tissue being the underlying mechanisms. These changes lead to the polarization of lung macrophages toward the M1 phenotype, augment the release of inflammatory factors, and result in the dysfunction of alveolar epithelial cells. Exosome inhibitors can regulate acute lung injury in mice by inhibiting the secretion of exosomes. These findings are expected to provide valuable therapeutic strategies for ALI.

Institutional Review Board Statement

This experiment has been approved by the Experimental Animal and Ethics Committee of Wannan Medical College (Approval number: LLSC-2021-119). This study was conducted in accordance with the The "3R" principle for reducing, replacing, and optimizing animal experiment.

Funding

This work was supported by the Anhui Provincial Natural Science Foundation(2108085MH300) and the Anhui Provincial Clinical Medical Research and Translational Project(202304295107020006,202304295107020001).

Disclosure

The authors report no conflicts of interest in this work.

References

1. Lin P, Gao R, Fang Z, et al. Precise nanodrug delivery systems with cell-specific targeting for ALI/ARDS treatment. *Int J Pharm.* 2023;644:123321. doi:10.1016/j.ijpharm.2023.123321
2. Lu Y, Liu D, Feng Q, Liu Z. Diabetic nephropathy: perspective on extracellular vesicles. *Front Immunol.* 2020;11:943. doi:10.3389/fimmu.2020.00943
3. Yang D, Zhang W, Zhang H, et al. Progress, opportunity, and perspective on exosome isolation - efforts for efficient exosome-based theranostics. *Theranostics.* 2020;10(8):3684–3707. doi:10.7150/thno.41580

4. Jiao Y, Zhang T, Zhang C, et al. Exosomal miR-30d-5p of neutrophils induces M1 macrophage polarization and primes macrophage pyroptosis in sepsis-related acute lung injury. *Crit Care*. 2021;25(1):356. doi:10.1186/s13054-021-03775-3
5. Xia L, Zhang C, Lv N, et al. AdMSC-derived exosomes alleviate acute lung injury via transferring mitochondrial component to improve homeostasis of alveolar macrophages. *Theranostics*. 2022;12(6):2928–2947. doi:10.7150/thno.69533
6. Cheng P, Li S, Chen H. Macrophages in lung injury, repair, and fibrosis. *Cells*. 2021;10(2):436. doi:10.3390/cells10020436
7. Chen L, Gu YJ, Zhang XG, et al. Macrophage microvesicle-derived circ_YTHDF2 in methamphetamine-induced chronic lung injury. *J Physiol*. 2023;601(22):5107–5128. doi:10.1113/JP284086
8. Dos Santos CC, Lopes-Pacheco M, English K, Rolandsson Enes S, Krasnodembskaya A, Rocco PRM. The MSC-EV-microRNAome: a perspective on therapeutic mechanisms of action in sepsis and ARDS. *Cells*. 2024;13(2):122. doi:10.3390/cells13020122
9. Huang X, Xiu H, Zhang S, Zhang G. The role of macrophages in the pathogenesis of ALI/ARDS. *Mediators Inflamm*. 2018;2018:1264913. doi:10.1155/2018/1264913
10. Frossard JL, Lenglet S, Montecucco F, et al. Role of CCL-2, CCR-2 and CCR-4 in cerulein-induced acute pancreatitis and pancreatitis-associated lung injury. *J Clin Pathol*. 2011;64(5):387–393. doi:10.1136/jcp.2010.088500
11. Cao X, Zhang C, Zhang X, Chen Y, Zhang H. MiR-145 negatively regulates TGFBR2 signaling responsible for sepsis-induced acute lung injury. *Biomed. Pharmacother*. 2019;111:852–858. doi:10.1016/j.biopha.2018.12.138
12. Letsiou E, Teixeira Alves LG, Fatykhova D, et al. Microvesicles released from pneumolysin-stimulated lung epithelial cells carry mitochondrial cargo and suppress neutrophil oxidative burst. *Sci Rep*. 2021;11(1):9529. doi:10.1038/s41598-021-88897-y
13. Rittirsch D, Huber-Lang MS, Flierl MA, Ward PA. Immunodesign of experimental sepsis by cecal ligation and puncture. *Nature Protocols*. 2008;4(1):31–36. doi:10.1038/nprot.2008.214
14. Liu D, Huang SY, Sun JH, et al. Sepsis-induced immunosuppression: mechanisms, diagnosis and current treatment options. *Military Med Res*. 2022;9(1):56. doi:10.1186/s40779-022-00422-y
15. Dolmatova EV, Forrester SJ, Wang K, et al. Endothelial Poldip2 regulates sepsis-induced lung injury via Rho pathway activation. *Cardiovasc Res*. 2022;118(11):2506–2518. doi:10.1093/cvr/cvab295
16. Mowery NT, Terzian WTH, Nelson AC. Acute lung injury. *Curr Probl Surg*. 2020;57(5):100777. doi:10.1016/j.cpsurg.2020.100777
17. Kumar V. Pulmonary innate immune response determines the outcome of inflammation during pneumonia and sepsis-associated acute lung injury. *Front Immunol*. 2020;11:1722. doi:10.3389/fimmu.2020.01722
18. Zhu T, Liao X, Feng T, et al. Plasma monocyte chemoattractant protein 1 as a predictive marker for sepsis prognosis: a prospective cohort study. *Tohoku J Exp Med*. 2017;241(2):139–147. doi:10.1620/tjem.241.139
19. Cavalcanti NV, Torres LC, da Matta MC, et al. Chemokine patterns in children with acute bacterial infections. *Scand J Immunol*. 2016;84(6):338–343. doi:10.1111/sji.12492
20. Rose CE Jr, Sung SS, Fu SM. Significant involvement of CCL2 (MCP-1) in inflammatory disorders of the lung. *Microcirculation*. 2003;10(3–4):273–288. doi:10.1038/sj.mn.7800193
21. Tang N, Yang Y, Xie Y, et al. CD274 (PD-L1) negatively regulates M1 macrophage polarization in ALI/ARDS. *Front Immunol*. 2024;15:1344805.
22. Crosby LM, Waters CM. Epithelial repair mechanisms in the lung. *Am J Physiol Lung Cell Mol Physiol*. 2010;298(6):L715–731. doi:10.1152/ajplung.00361.2009
23. Qian BZ, Li J, Zhang H, et al. CCL2 recruits inflammatory monocytes to facilitate breast-tumour metastasis. *Nature*. 2011;475(7355):222–225. doi:10.1038/nature10138
24. Aggarwal NR, King LS, D'Alessio FR. Diverse macrophage populations mediate acute lung inflammation and resolution. *Am J Physiol Lung Cell Mol Physiol*. 2014;306(8):L709–725. doi:10.1152/ajplung.00341.2013
25. Singh S, Anshita D, Ravichandiran V. MCP-1: function, regulation, and involvement in disease. *Int Immunopharmacol*. 2021;101(Pt B):107598. doi:10.1016/j.intimp.2021.107598
26. Matthay MA, Zemans RL, Zimmerman GA, et al. Acute respiratory distress syndrome. *Nat Rev Dis Primers*. 2019;5(1):18. doi:10.1038/s41572-019-0069-0
27. Wahlund CJE, Eklund A, Grunewald J, Gabrielsson S. Pulmonary extracellular vesicles as mediators of local and systemic inflammation. *Front Cell Develop Biol*. 2017;5:39. doi:10.3389/fcell.2017.00039
28. Hovhannisyan L, Czechowska E, Gutowska-Owsiak D. The role of non-immune cell-derived extracellular vesicles in allergy. *Front Immunol*. 2021;12:702381. doi:10.3389/fimmu.2021.702381
29. Barile L, Vassalli G. Exosomes: therapy delivery tools and biomarkers of diseases. *Pharmacol Ther*. 2017;174:63–78. doi:10.1016/j.pharmthera.2017.02.020
30. Matsumoto H, Ogura H, Shimizu K, et al. The clinical importance of a cytokine network in the acute phase of sepsis. *Sci Rep*. 2018;8(1):13995. doi:10.1038/s41598-018-32275-8
31. Zhao J, Yu H, Liu Y, et al. Protective effect of suppressing STAT3 activity in LPS-induced acute lung injury. *Am J Physiol Lung Cell Mol Physiol*. 2016;311(5):L868–L880. doi:10.1152/ajplung.00281.2016
32. Tahyra ASC, Calado RT, Almeida F. The role of extracellular vesicles in COVID-19 pathology. *Cells*. 2022;11(16):2496. doi:10.3390/cells11162496
33. Soni S, O'Dea KP, Tan YY, et al. ATP redirects cytokine trafficking and promotes novel membrane TNF signaling via microvesicles. *FASEB J*. 2019;33(5):6442–6455. doi:10.1096/fj.201802386R
34. Kieler M, Hofmann M, Schabbauer G. More than just protein building blocks: how amino acids and related metabolic pathways fuel macrophage polarization. *FEBS J*. 2021;288(12):3694–3714. doi:10.1111/febs.15715
35. Liang L, Xu W, Shen A, et al. Inhibition of YAP1 activity ameliorates acute lung injury through promotion of M2 macrophage polarization. *MedComm*. 2023;4(3):e293. doi:10.1002/mco.2.293
36. Wang L, Wang D, Zhang T, Ma Y, Tong X, Fan H. The role of immunometabolism in macrophage polarization and its impact on acute lung injury/acute respiratory distress syndrome. *Front Immunol*. 2023;14:1117548.
37. Bardi GT, Smith MA, Hood JL. Melanoma exosomes promote mixed M1 and M2 macrophage polarization. *Cytokine*. 2018;105:63–72. doi:10.1016/j.cyto.2018.02.002

38. Sanacora S, Chang TP, Vancurova I. Chromatin immunoprecipitation analysis of bortezomib-mediated inhibition of NFκB recruitment to IL-1β and TNFα gene promoters in human macrophages. *Methods Mol Biol.* 2014;1172:315–327.
39. Cossarizza A, Chang HD, Radbruch A, et al. Guidelines for the use of flow cytometry and cell sorting in immunological studies (third edition). *Eur J Immunol.* 2021;51(12):2708–3145. doi:10.1002/eji.202170126

Journal of Inflammation Research

Publish your work in this journal

The Journal of Inflammation Research is an international, peer-reviewed open-access journal that welcomes laboratory and clinical findings on the molecular basis, cell biology and pharmacology of inflammation including original research, reviews, symposium reports, hypothesis formation and commentaries on: acute/chronic inflammation; mediators of inflammation; cellular processes; molecular mechanisms; pharmacology and novel anti-inflammatory drugs; clinical conditions involving inflammation. The manuscript management system is completely online and includes a very quick and fair peer-review system. Visit <http://www.dovepress.com/testimonials.php> to read real quotes from published authors.

Submit your manuscript here: <https://www.dovepress.com/journal-of-inflammation-research-journal>

Dovepress
Taylor & Francis Group